Proceedings of the 2016 Joint Rail Conference
JRC2016
April 12-15, 2016, Columbia, SC, USA

JRC2016-5802

FATIGUE ANALYSIS OF RAIL-HEAD-TO-WEB FILLET AT BOLTED RAIL JOINT UNDER VARIOUS IMPACT WHEEL LOAD FACTORS AND SUPPORT CONFIGURATIONS

Kaijun Zhu, J. Riley Edwards, Yu Qian, and Bassem O. Andrawes
University of Illinois at Urbana-Champaign
Department of Civil and Environmental Engineering
Rail Transportation and Engineering Center (RailTEC)
205 N Mathews Ave
Urbana, IL, United States 61801

ABSTRACT

As one of the weakest locations in the track superstructure, the rail joint encounters different types of defects and failures, including rail bolt-hole cracking, rail head-web cracking or separation, broken or missing bolts, and joint bar cracking. The defects and failures are mainly initiated by the discontinuities of both geometric and mechanical properties due to the rail joint, and the high impact loads induced by the discontinuities. Continuous welded rail (CWR) overcomes most disadvantages of the rail joints. However, a large number of rail joints still exist in North American Railroads for a variety of reasons, and bolted joints are especially prevalent in early-built rail transit systems. Cracks are often found to initiate in the area of the first bolt-hole and rail-head-to-web fillet (upper fillet) at the rail end among bolted rail joints, which might cause further defects, such as rail breaks or loss of rail running surface. Previous research conducted at the University of Illinois at Urbana-Champaign (UIUC) has established an elastic static Finite Element (FE) model to study the stress distribution of the bolted rail joint with particular emphasis on rail end bolt-hole and upper fillet areas. Based on the stress calculated from the FE models, this paper focuses on the fatigue performance of upper fillet under different impact wheel load factors and crosstie support configurations. Preliminary results show that the estimated fatigue life of rail end upper fillet decreases as impact factor increases, and that a supported joint performs better than a suspended joint on upper fillet fatigue life.

INTRODUCTION

Rail joints are used to connect two adjacent rails. Typically, a pair of joint bars are placed on each side of the two adjacent rail ends, fixed with at least four bolts. Two main categories are used to classify rail joints: insulated joints (IJs) and bolted joints. Bolted joints can be further categorized into compromise joints and standard joints. Compromise joints are used when two rails with dissimilar sections need to be connected, while standard joints are installed with two similar rail sections. Standard joints are mostly seen in bolted-joint rail (BJR) track, however, they can be observed in continuously welded rail (CWR) track as well, which are used as temporary joints to connect long CWR strings before welding [1].

In railroad track superstructure, the rail joint is treated as one of the weakest spots, mainly because of its discontinuities of both geometric and mechanical properties. Geometric discontinuity includes rail gap, height mismatch, and dip angle (Figure 1) [2]. The smaller section area and lower bending stiffness of joint bars, compared to the rail itself, leads to the discontinuity of mechanical properties (Figure 2) [3]. Those discontinuities can cause high wheel impact loads, which might lead to rail end batter, loosened bolts, deteriorated support condition, and excessive deflection. Such defects can potentially lead to the following failure modes: bolt-hole cracks, head-web separation, bent or broken bolts, and cracked or broken joint bars [4, 5].

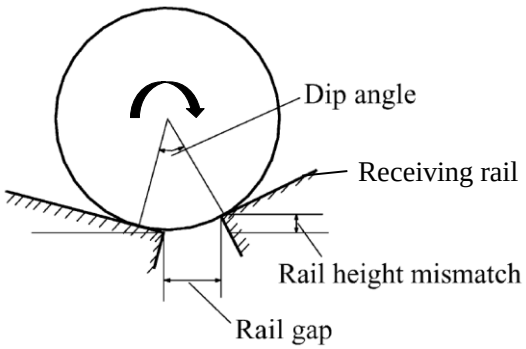

Figure 1. Discontinuity of Geometry at Rail Joint [2]

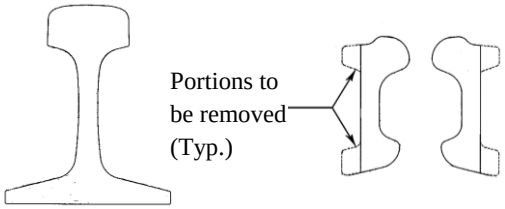

Figure 2. Discontinuity of Mechanical Properties [3]

In the rail joint area, two of the most common defects are rail bolt-hole cracks and head-web separations (Figures 3 and 4). These defects can lead to rail breaks or loss of rail running surface.

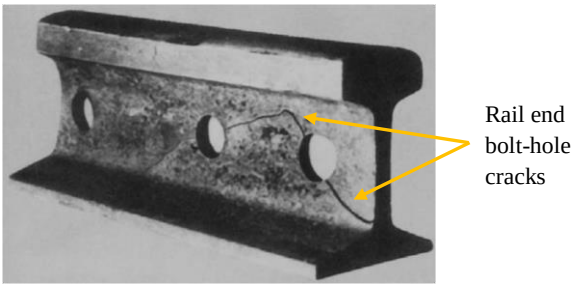

Figure 3. Typical Rail End Bolt-Hole Crack [2]

Bolt-hole crack typically originates at the very end bolt-hole of the receiving rail, and at an angle that is approximately 45 °to the neutral axis of the rail [6-8] (Figure 3). Based on previous research, in BJR track, the bolt-hole cracks are typically generated by the positive shear stress around the bolt-hole. Such shear stress increases with the wheel-rail impact load, and the stress-concentration effect of the hole can cause further amplification [9, 10]. In CWR track, on the other hand, the primary cause for the bolt-hole cracks in temporary joints is the thermal-induced longitudinal stresses [8, 11].

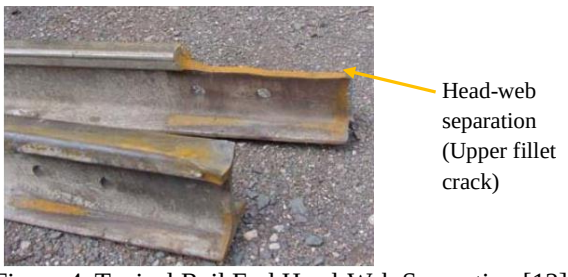

Figure 4. Typical Rail End Head-Web Separation [12]

Rail head-web separation is a progressive horizontal defect initiating from the upper fillet area between rail head and web, which may occur at rail joints (Figure 4). Typically at rail joint areas, head-web separation initiates at the rail end, gradually develops over bolt-holes, and finally reaches the rail running surface. The primary originator for this defect is a fatigue failure caused by high magnitude repeated vertical impact loads and deflections, or the improper contact between rail and joint bars due to low quality of installation [3].

In addition, the initial cracks at both rail end bolt-hole and upper fillet areas are difficult to observe, because they are behind joint bars such that the effectiveness of human (visual) or machine-vision-based inspection methods is restricted. Additionally, limited information has been found on ultrasonic inspection of bolted rail joints. Accordingly, a better understanding of material fatigue life at rail end bolt-hole and upper fillet areas could possibly help improve the efficiency and accuracy of crack detection and maintenance at rail joints.

Previous research in the Rail Transportation and Engineering Center (RailTEC) at the University of Illinois at Urbana-Champaign (UIUC) focused on FE-based parametric analysis of the stress distribution around the rail end bolt-hole and at the upper fillet area. This paper will follow one branch of the previous work and study the fatigue performance of rail end upper fillet under various impact wheel load factors and crosstie support configurations. Preliminary results of estimated fatigue life of the rail end upper fillet will be presented based on findings from a fatigue parametric study. The fatigue analysis for rail end bolt-hole area will be presented in a future publication.

METHODOLOGY

A parametric study was carried out to investigate the fatigue performance of standard bolted joint with respect to upper fillet crack issues. All of the constants, variables, and outputs that were considered in this fatigue parametric study are listed in Table 1.

Table 1. Fatigue Parametric Study Matrix

Constants	
Rail Section	115 RE
Crosstie Spacing	22.5 in
Track Modulus	4,000 psi for resilient plate
Bolt Preloading	22,000 psi per bolt
Static Wheel Load	16,500 lb per wheel
Wheel Load Position	above rail end
Variables	
Crosstie Support Configuration	(A) suspended (B) supported (C) broken plate
Impact Wheel Load Factor	1.33 2.0 3.0
Key Outputs	
Estimated Fatigue Life at Rail End Upper Fillet	

As shown in Table 1, the bolted rail joint adopted in this study is installed in 115 RE rail track with track modulus of 4,000 psi and average crosstie spacing of 22.5 in. The rail section, 115 RE, is currently used for both freight railroad and rail transit systems in North America. The track stiffness of 4,000 psi was provided by New York City Transit Authority (NYCTA) from a field test, and this value was acquired specifically from the system with resilient plates between the rail and crossties. The bolt preloading of 22,000 psi was selected according to Chapter 5, Section 5.5 of the American Railway Engineering and Maintenance-of-way Association (AREMA) Manual for Railway Engineering (hereafter referred to as the "AREMA Manual") [3]. The static wheel load of 16,500 lb per wheel was provided by NYCTA as well. The wheel load position was determined based on previous research conducted at UIUC, which indicates that the rail end upper fillet stress reaches its maximum value when the wheel is at the rail end [13].

The three types of crosstie support configurations are shown in Figure 5. Case (A) "suspended" and (B) "supported" are two of the most representative crosstie support configurations that can be observed for rail joints in the field. Case (C) "broken plate" is the worst-case scenario in this study, and was used to provide an upper bound on the study of joint fatigue.

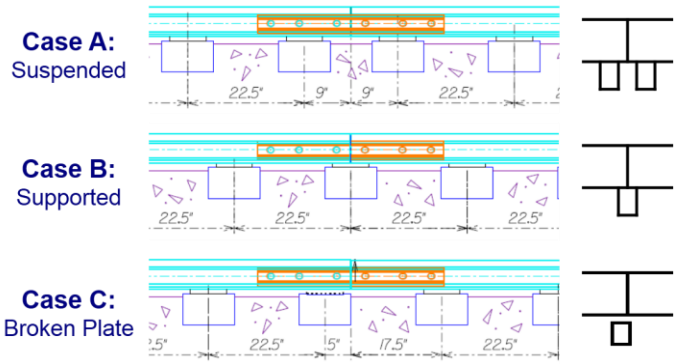

Figure 5. Three Cases of Crosstie Support Configurations

The minimum impact factor of 1.33 was suggested by NYCTA, while the maximum impact factor of 3.0 was decided based on the AREMA Manual, which suggests a 200% increase over static vertical loads to estimate the dynamic effect of wheel and rail irregularities [3].

The key output for this parametric study is the estimated fatigue life at rail end upper fillet area. Details of the FE-based parametric analysis and parameters listed in Table 1 have been provided elsewhere [13].

Fatigue Analysis Procedures

The fatigue analysis procedure used in this study is illustrated in Figure 6. First, the stresses calculated from the FE-based parametric analysis [13] using *Abaqus* are required, and they play a key role on obtaining rational estimated fatigue life. Those stresses could then be read by another commercially available software *fe-safe* to perform the fatigue parametric study. In addition to the stress results, information of loading history and material properties, as well as the selection of the methods of fatigue algorithm and mean stress correction, are of great importance during the fatigue analysis, and will be introduced in detail in the following sections.

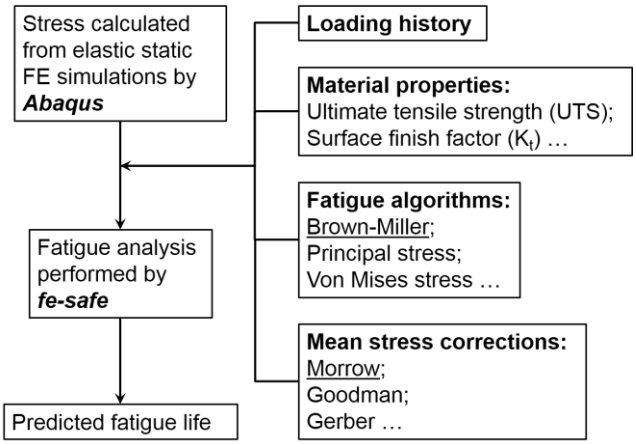

Figure 6. Fatigue Analysis Procedure

Loading History

Loading history defines the stresses that the structure experiences during the fatigue analysis, which normally consists of the stresses calculated from FE analysis with a load factor function. The stresses applied in this fatigue parametric study have been obtained from previous study [13] and can be input directly into *fe-safe*. Those stresses would be utilized as the base load, and could be factored using a load factor function. In this analysis, the load factor function was set as a sinusoidal function as plotted in Figure 7, with a magnitude varying from 0 to 1. Each cycle in this curve represents a pass of the wheel over the rail joint, so that the stress among the joint components would gradually increase to its maximum and then decrease to zero within one cycle. The estimated fatigue life is the total cycles of the loading that the system has experienced before damage occurs, namely, the total number of wheels passing over the rail joint before damage initiates.

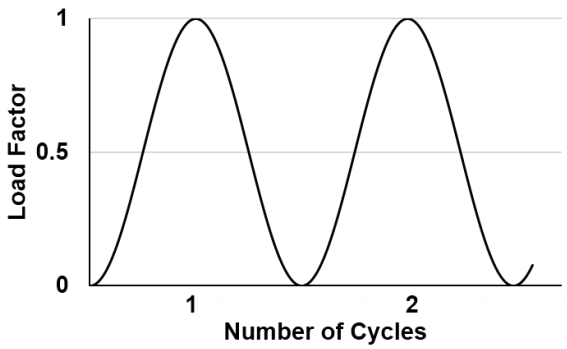

Figure 7. Load Factor Function Applied in Fatigue Analysis

Material Properties

Based on a test report provided by NYCTA, the ultimate tensile strength (UTS) of the rail steel is around 177.0 ksi. Other necessary material properties used for the fatigue analysis are listed in Table 2 and those values are based on estimation and typical values from literature [14].

Table 2. Material Properties for Fatigue Analysis

Parameters	Symbols	Values
Ultimate Tensile Strength	UTS	177.0 ksi
Strength at 10^5 cycles	-	112.2 ksi
Strength at 10^7 cycles (Fatigue Limit)	-	61.5 ksi
Young's Modulus	E	29,000 ksi
Poisson's Ratio	ν	0.33
Strain Hardening Coefficient	K'	292.0 ksi
Strain Hardening Exponent	n'	0.15
Fatigue Strength Coefficient	σ_f'	265.5 ksi
Fatigue Strength Exponent	b	-0.087
Fatigue Ductility Coefficient	ε_f'	0.361
Fatigue Ductility Exponent	c	-0.58
Surface Finish Factor	K_t	1.38

The fatigue limit represents a cyclic stress amplitude below which the material does not fail and can be cycled indefinitely [15]. For ductile steel specifically, the fatigue limit is the strength of the material at 10^7 cycles of loading. In other words, if the steel structure system could experience at least 10^7 cycles of loadings without cracking or other damages, it is assumed that no fatigue damage would occur in the future under the exact same loading conditions.

Fatigue Algorithm

The Brown-Miller criterion was selected for this specific fatigue analysis, which gives the most realistic fatigue life estimates for ductile metals [16]. The Brown-Miller equation suggests that the maximum fatigue damage occurs on the plane which experiences the maximum shear strain amplitude, and that damage is a function of both this shear strain amplitude ($\Delta\gamma_{max}/2$) and the normal strain amplitude ($\Delta\varepsilon_n/2$), due to the combined action of shear and normal strain reducing fatigue life. Accordingly, different from the conventional strain-life equation (Equation 1), the Brown-Miller equation (Equation 2) alters the left hand side with the shear strain amplitude and normal strain amplitude [16].

$$\frac{\Delta\varepsilon}{2} = \frac{\sigma_f'}{E}(2N_f)^b + \varepsilon_f'(2N_f)^c \quad (1)$$

where, $\Delta\varepsilon/2$ = applied strain amplitude
$2N_f$ = endurance in reversals
σ_f' = fatigue strength coefficient
ε_f' = fatigue ductility coefficient
b = fatigue strength exponent
c = fatigue ductility exponent

$$\frac{\Delta\gamma_{max}}{2} + \frac{\Delta\varepsilon_n}{2} = C_1\frac{\sigma_f'}{E}(2N_f)^b + C_2\varepsilon_f'(2N_f)^c \quad (2)$$

where, $\Delta\gamma_{max}/2$ = shear strain amplitude
$\Delta\varepsilon_n/2$ = normal strain amplitude
C_1 = 1.65 (constant)
C_2 = 1.75 (constant)
σ_f', ε_f', b, and c are the same as in Equation 1

The constants C_1 = 1.65 and C_2 = 1.75 were derived on the assumption that cracks initiate on the plane of maximum shear strain. However, for complex variable amplitude loading, it was found that better agreement with test results was obtained by assuming that the most damaged plane was the one that produced the highest value of $\frac{\Delta\gamma_{max}}{2} + \frac{\Delta\varepsilon_n}{2}$. For that case, the constants C_1 and C_2 will have slightly different values on this plane. Nevertheless, the values shown in Equation 2 could be applied generally [16].

Mean Stress Correction

Typically, it is common for a service load history to have a non-zero mean stress, σ_m, which is defined in Equation 3. The fatigue performance would vary as the mean stress changes. The influence of mean stress can be characterized as the influence of stress ratio, R, the ratio of minimum stress to maximum stress in fatigue load cycle (Equation 4).

$$\sigma_m = \frac{\sigma_{max}+\sigma_{min}}{2} \quad (3)$$

$$R = \frac{\sigma_{min}}{\sigma_{max}} \quad (4)$$

$$\sigma_a = \frac{\sigma_{max}-\sigma_{min}}{2} \quad (5)$$

where, σ_m = mean stress
R = stress ratio
σ_a = stress amplitude
σ_{max} = maximum stress
σ_{min} = minimum stress

The effect of the mean stress on fatigue life is shown in Figure 8. It can be observed that the endurance cycles, N_f, increases as the applied stress amplitude, σ_a (Equation 5), decreases. There are two functions plotted in this figure, corresponding to the cases with zero minimum stress (R = 0) and with zero mean stress (R = -1), respectively. The function with R = 0 is overall below the other function with R = -1, which illustrates that a larger mean stress in tension would lead to a shorter life. Additionally, the functions become parallel to the x-axis when the endurance cycles reach 10^7, representing the condition in which no fatigue failure would occur.

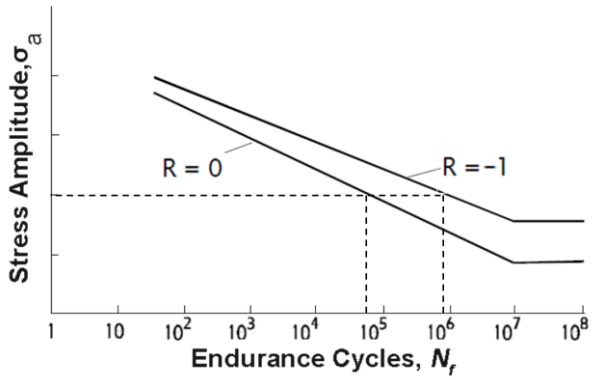

Figure 8. Effect of the Mean Stress on Fatigue Life [16]

The Morrow mean stress correction is recommended for Brown-Miller criterion [16]. After the Morrow mean stress correction is applied, the Brown Miller equation (Equation 2) becomes Equation 6, with a corrected elastic term by subtracting the mean normal stress on the plane, $\sigma_{n,m}$.

$$\frac{\Delta\gamma_{max}}{2} + \frac{\Delta\varepsilon_n}{2} = 1.65\frac{(\sigma_f' - \sigma_{n,m})}{E}(2N_f)^b + 1.75\varepsilon_f'(2N_f)^c \qquad (6)$$

where, $\sigma_{n,m}$ = mean normal stress

$\Delta\gamma_{max}/2$, $\Delta\varepsilon/2$, σ_f', ε_f', b, and c are the same as those in Equations 1 and 2.

PRELIMINARY RESULTS AND DISCUSSION

With the loading history, material properties, fatigue algorithm, and mean stress correction method properly assigned, the fatigue analyses were then performed. The results of this parametric study were organized and presented as follows. The estimated fatigue life at rail end upper fillet varies with different impact wheel load factors and crosstie support configurations (Figure 9).

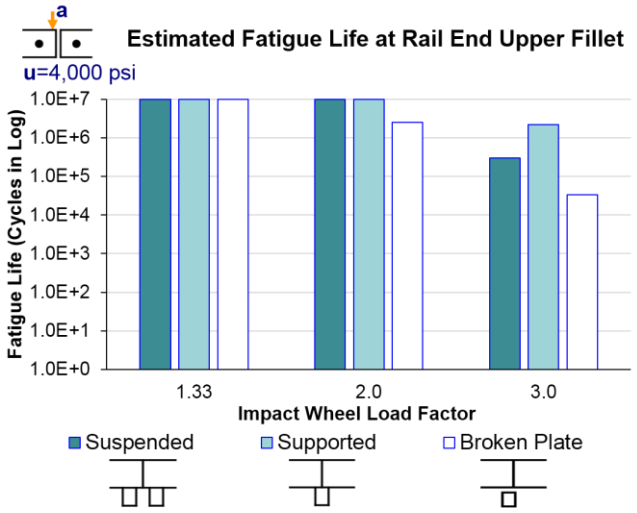

Figure 9. Estimated Fatigue Life at Rail End Upper Fillet

The effect of various wheel load impact factors can be observed in Figure 9. When the impact wheel load factor increases, the estimated fatigue life at the rail end upper fillet decreases for all three crosstie support configurations. This is due to the increasing stress and deflection at the rail joint as impact wheel load factors increase. More specifically, the endurance cycles reach 10^7 cycles for all three crosstie support configurations, indicating that no fatigue damage occurs at rail end upper fillet when the impact wheel load factor is at 1.33. When the impact wheel load factor reaches 3.0, the estimated fatigue life at rail end upper fillet decreases and becomes lower than 10^7 cycles, and fatigue damage is likely to occur at upper fillet for all the three crosstie support configurations.

Crosstie support configuration also plays a significant role as shown in Figure 9. Rail joints with "suspended" and "supported" configurations would not be likely to have fatigue failure at upper fillet area when the impact wheel load factor remains less than 2.0, while it is likely for rail joint to experience upper fillet damage with a broken plate configuration under the impact wheel load factor of 2.0. A clearer comparison of the three crosstie support configurations could be made when the impact wheel load factor was set to be 3.0, where it can be seen that the rail joint with "supported" configuration performs better than the rail joint with "suspended" configuration with respect to the fatigue life at upper fillet area, and the rail joint with "broken plate" configuration has the shortest estimated upper fillet fatigue life.

Palmgren-Miner Rule

The results shown previously are made under the assumption that the impact wheel load factors are fixed at 1.33, 2.0, or 3.0, respectively. In the field, however, the impact wheel load factor varies from wheel to wheel, which could influence the prediction of fatigue life and needs to be considered in this study by adopting the Palmgren-Miner rule [15]. The Palgrem-Miner rule is a linear cumulative-damage theory as shown in Equation 7. It suggests that the damage occurs when the summation of all life fractions reaches unity. In this research, three life fractions are considered, which are labeled with the corresponding impact wheel load factors.

$$\sum\frac{n_i}{N_i} = \frac{n_{1.33}}{N_{1.33}} + \frac{n_{2.0}}{N_{2.0}} + \frac{n_{3.0}}{N_{3.0}} = 1 \text{ (Unity)} \qquad (7)$$

where, N_i = fatigue life corresponding to impact factor i

n_i = number of cycles carried out at impact factor i

ni/Ni = life fraction corresponding to impact factor i

Table 3. Example Results for Rail Joint with Broken Plate

Impact Factor	Fatigue Life (Cycles, N_i)	Elapsed Life (Cycles, n_i)
1.33	$N_{1.33} = 1.0 \times 10^7$ (No damage)	$n_{1.33}$
2.0	$N_{2.0} = 2.53 \times 10^6$	$n_{2.0}$
3.0	$N_{3.0} = 3.29 \times 10^4$	$n_{3.0}$

Note: When using Equation 7, $N_{1.33}$ should be substituted in as infinity.

Take the rail joint with broken plate configuration as an example, the results of which are shown in Table 3. The fatigue lives (N_i) are estimated using the methods described earlier. With a certain number of passing trains, the elapsed lives (n_i) could be estimated if the probability distribution of impact wheel load factors could be captured in field test. Equation 7 could then be used to predict the number of trains that the rail joint can hold before damage occurs at the rail end upper fillet. The fatigue life corresponding to impact wheel load factor of 1.33 ($N_{1.33}$) should be substituted in Equation 7 as infinity, and the first portion of that equation would equal zero, such that the running wheels with impact factor of 1.33 would cause no damage to the upper fillet.

CONCLUSIONS

This paper focuses on the influence of impact wheel load factor and crosstie support configuration on fatigue performance at the rail end upper fillet area among bolted rail joints. A parametric study was performed using a fatigue analysis software, *fe-safe*, based on the stresses calculated in prior work. According to the results from this fatigue parametric study, the following conclusions can be drawn:

- The estimated fatigue life of rail end upper fillet decreases as the impact wheel load factor increases. Under the fatigue analysis assumptions and criteria in this study, fatigue damage would not be likely to occur if the impact wheel load factor is below 1.33, even under the worst case scenario with "broken plate" configuration;
- The "supported" rail joint configuration performs better than the "suspended" rail joint configuration with respect to the fatigue life at upper fillet area, and the rail joint with "broken plate" configuration has the shortest estimated upper fillet fatigue life among the three crosstie support configurations.
- The understanding of the probability distribution of impact wheel load factors in the field could help predict the fatigue life in terms of a number of passing trains.
- The estimated fatigue life from this model will need to be verified through experiments before these results can be accurately applied into field practice.

ACKNOWLEDGMENTS

This research was supported by WSP | Parsons Brinckerhoff and New York City Transit (NYCTA), and the National University Rail (NURail) Center, and was based on background information that was provided under a broader research program for WSP | Parsons Brinckerhoff and NYCTA. The authors would like to thank WSP | Parsons Brinckerhoff, NYCTA Inspections and Testing, and NYCTA Track Engineering for providing leadership and oversight for the broader work that this paper was associated with. The authors would also like to thank Prof. Don Uzarski and Michael Yang from the University of Illinois at Urbana-Champaign (UIUC), and Michael Carolan from Volpe National Transportation Center for their assistance and advice. The opinions expressed in this article are solely those of the authors and do not represent the opinions of the funding agency. J. Riley Edwards has been supported in part by grants to the UIUC Rail Transportation and Engineering Center (RailTEC) from CN, and Hanson Professional Services.

REFERENCES

[1] Akhtar, M. N. and D. D. Davis. 2013. Load Environment of Rail Joint Bars- Phase I: Effects of Track Parameters on Rail Joint Stresses and Crack Growth. Final Report, DOT/FRA/ORD-13/24.

[2] Wen, Z., X. Jin, and W. Zhang. 2005. Contact-Impact Stress Analysis of Rail Joint Region Using the Dynamic Finite Element Method. *Wear*, Volume 258, Issue 7, pp. 1301-1309.

[3] American Railway Engineering and Maintenance-of-Way Association. *Manual for Railway Engineering*. 2015.

[4] Jeong, D.Y., R. Bruzek, and A. Tajaddini. 2014 Engineering Studies on Joint Bar Integrity, Part I: Field Surveys and Obvsered Failure Modes. Proceedings of the 2014 Joint Rail Conference, JRC 2014-3706, April 2014, Colorado Springs, CO.

[5] Carolan, M.E., D.Y. Jeong, and A.B. Perlman. 2014. Engiheering Studies on Joint Bar Integrity, Part II: Finite Element Analysis. Proceedings of the 2014 Joint Rail Conference, JRC 2014-3708, April 2014, Colorado Springs, CO.

[6] Orringer, O., J.M. Morris, and R.K. Steele. 1984. Applied Research on Rail Fatigue and Fracture in the United States. *Theoretical and Applied Fracture Mechanics*, Volume 1, Issue 1, pp. 23-49.

[7] Jeong, D. Y. 2001. *Progress in Rail Integrity Research*. Final Report, DOT/FRA/ORD-01/18.

[8] Mayville, R. A. and P. D. Hilton. 1984. Fracture Mechanics Analysis of a Rail-End Bolt-Hole Crack. *Theoretical and Applied Fracture Mechanics*, Volume 1, Issue 1, pp. 51-60.

[9] Mayville, R. A. and R. G. Stringfellow. 1993. *Development and Application of Rail Defect Fracture Models to Assess Remedial Actions*. Final Report, DOT/FRA/ORD-93/33.

[10] Mayville, R. A. and R. G. Stringfellow. 1995. Numerical Analysis of a Railroad Bolt-Hole Fracture Problem. *Theoretical and Applied Fracture Mechanics*, Volume 24, Issue 1, pp. 1-12.

[11] Sih, G.C. and D.Y. Tzou. 1985. Rail-End Bolt-Hole Fatigue Crack in Three Dimensions. *Theoretical and Applied Fracture Mechanics*, Volume 3, Issue 2, pp. 97-111.

[12] Federal Railroad Administration. *Track Inspector Rail Defect Reference Manual*. 2015.

[13] Zhu, K., R. Edwards, Y. Qian, and B. Andrawes. 2016. Finite Element Analysis of the Effects of Bolt Condition on Bolted Rail Joints Stresses. *Transportation Research Record: Journal of the Transportation Research Board* (Accepted)

[14] Fe-safe. 2014. *Material Database.* Safe Technology Limited.
[15] Meyers, M. A., and K. K. Chawla. 2009. *Mechanical behavior of materials.* Volume 2. Cambridge University Press.
[16] Fe-safe. 2002. *Fatigue Theory Reference Manual.* Volume 2. Safe Technology Limited.